Structural and Spectroscopic Comparisons between (μ-Oxo)- and (μ-Hydroxo)bis(μ-carboxylato)diiron(III) Complexes That Contain All-Oxygen-Donor Ligands

Tadashi J. Mizoguchi,[†] Roman M. Davydov,*[,‡] and Stephen J. Lippard*[,†]

Departments of Chemistry, Massachusetts Institute of Technology, Cambridge, Massachusetts 02139, and Northwestern University, Evanston, Illinois 60208

Received March 16, 1999

Treatment of the (μ-oxo)bis(μ-carboxylato)diiron(III) complex $[Fe_2(\mu\text{-}O)(\mu\text{-}XDK)(CH_3OH)_6]^{2+}$, where XDK^{2-} = the dianion of *m*-xylylenediamine bis(Kemp's triacid imide), with 2 equiv of 1,1,1,5,5,5-hexafluoroacetylacetone (hfacH) and Et_3N led to substitution of two methanol ligands by a bidentate $hfac^-$ anion at each metal center. The green bis(aqua) complex $[Fe_2(\mu\text{-}O)(\mu\text{-}XDK)(hfac)_2(H_2O)_2]$ (**3**) was crystallographically characterized and presents water ligands bound trans to the bridging oxo group. Omission of Et_3N from the above synthesis afforded an orange adduct, which is assigned as the (μ-hydroxo)(μ-XDK)bis(hfac)diiron(III) complex. Analytically pure samples of this $[Fe_2(\mu\text{-}OH)(\mu\text{-}XDK)(hfac)_2(H_2O)_2]^+$ (**4**) cation were obtained as the salt of the noncoordinating anion tetrakis(3,5-bis(trifluoromethyl)phenyl)borate. Protonation of the oxo bridge in compound **3** leads to significant structural changes that are localized to the {Fe−O−Fe} core. The optical spectrum of **3** contains a broad ligand-field transition centered ~590 nm, a band that is noticeably absent in **4**. The 77 K Mössbauer spectra of **3** and **4** appear as doublets with similar isomer shifts ($\delta \approx 0.5$ mm s^{-1}) but very different quadrupole splittings (ΔE_Q = 1.68 and 0.58 mm s^{-1} for **3** and **4**, respectively). When samples of **3** and **4** were subjected to γ-ray-induced cryoreduction, EPR-active species with *g*-values < 2 were generated. We attribute these signals to the formation of the corresponding mixed-valence $Fe^{II}Fe^{III}$ forms. The signal derived from **3** is narrowly dispersed ($g_{av} = 1.90$), whereas the one from **4** is more broadly dispersed ($g_{av} = 1.74$). Crystal data for $\mathbf{3}\cdot H_2O\cdot 1.5CH_3CN$: triclinic, *P*1, $a = 13.9442(3)$ Å, $b = 15.2151(4)$ Å, $c = 15.7164(3)$ Å, $\alpha = 109.032(1)°$, $\beta = 97.975(1)°$, $\gamma = 115.697(1)°$, $V = 2682.4(1)$ Å^3, $Z = 2$, $T = -85$ °C.

Introduction

Understanding the relationship between structure and reactivity of metalloproteins remains a significant challenge in bioinorganic chemistry. Within the context of carboxylate-bridged diiron proteins,[1−3] the reversible dioxygen-binding properties of hemerythrin (Hr) can be contrasted to the irreversible dioxygen-activating chemistry exhibited by enzymes such as methane monooxygenase (MMO) and ribonucleotide reductase (RNR). Examination of the active-site structures of a series of these proteins reveals that the dioxygen-activating enzymes generally contain a greater number of carboxylate ligands, and the potential importance of a relatively oxygen- and anion-rich coordination environment as a means to stabilize high-valent iron intermediates has been noted.[4] Recent efforts to reproduce these active-site features of carboxylate-bridged diiron proteins through careful exercises in ligand design have yielded synthetic models of Hr[5] and MMO/RNR[6,7] that exhibit functionally relevant structural and reactivity properties.

The diiron compound $[Fe_2(\mu\text{-}O)(\mu\text{-}O_2CCH_3)_2\{[OP(OEt)_2]_3Co(C_5H_5)\}_2]$ (**1**)[8] represents the first and still rare example of a (μ-oxo)bis(μ-carboxylato)diiron(III) complex that contains solely oxygen-donating ligands. This complex exhibits magnetic and spectroscopic properties that are distinct from those of more commonly encountered (μ-oxo)bis(μ-carboxylato)diiron(III) complexes, which generally bear terminal ligands containing either mixed oxygen/nitrogen or all nitrogen donors.[9] For example, the $^6A_1 \rightarrow [^4T_2]({}^4G)$ d−d transition in **1** occurs at relatively high energies ($\lambda_{max} = 569$ nm in CH_3CN) owing to the weak ligand-field strength of the facially coordinating $\{[OP(OEt)_2]_3Co(C_5H_5)\}^-$ ligand.[8]

To examine the chemical consequences afforded by such an oxygen-only and highly anionic coordination sphere, we have employed the cationic (μ-oxo)bis(μ-carboxylato)diiron(III) complex $[Fe_2(\mu\text{-}O)(\mu\text{-}XDK)(CH_3OH)_6]^{2+}$ (**2**),[10] where XDK^{2-} = the dianion of *m*-xylylenediamine bis(Kemp's triacid imide),[11,12] as a scaffold for binding exogenous donors through exchange of the labile methanol ligands. An analogous approach was employed to synthesize the first well-characterized examples

[†] Massachusetts Institute of Technology.
[‡] Northwestern University.

(1) Feig, A. L.; Lippard, S. J. *Chem. Rev.* **1994**, *94*, 759−805.
(2) Wallar, B. J.; Lipscomb, J. D. *Chem. Rev.* **1996**, *96*, 2625−2657.
(3) Kurtz, D. M., Jr. *JBIC* **1997**, *2*, 159−167.
(4) Nordlund, P.; Eklund, H. *Curr. Opin. Struct. Biol.* **1995**, *5*, 758−766.
(5) Mizoguchi, T. J.; Lippard, S. J. *J. Am. Chem. Soc.* **1998**, *120*, 11022−11023.
(6) Lee, D.; Lippard, S. J. *J. Am. Chem. Soc.* **1998**, *120*, 12153−12154.
(7) Hagadorn, J. R.; Que, L., Jr.; Tolman, W. B. *J. Am. Chem. Soc.* **1998**, *120*, 13531−13532.
(8) Feng, X.; Bott, S. G.; Lippard, S. J. *J. Am. Chem. Soc.* **1989**, *111*, 8046−8047.
(9) Kurtz, D. M., Jr. *Chem. Rev.* **1990**, *90*, 585−606.
(10) Watton, S. P.; Masschelein, A.; Rebek, J., Jr.; Lippard, S. J. *J. Am. Chem. Soc.* **1994**, *116*, 5196−5205.
(11) Rebek, J., Jr.; Marshall, L.; Wolak, R.; Parris, K.; Killoran, M.; Askew, B.; Nemeth, D.; Islam, N. *J. Am. Chem. Soc.* **1985**, *107*, 7476−7481.
(12) Marshall, L.; Parris, K.; Rebek, J., Jr.; Luis, S. V.; Burguete, M. I. *J. Am. Chem. Soc.* **1988**, *110*, 5192−5193.

10.1021/ic990303y CCC: $18.00
Published on Web 08/20/1999

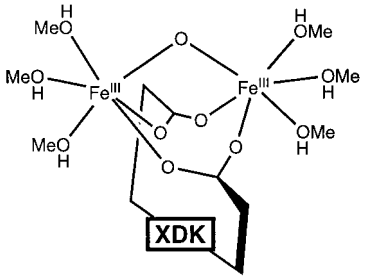

$[Fe_2(\mu\text{-}O)(\mu\text{-}XDK)(MeOH)_6]^{2+}$ (**2**)

of pseudohalide-bound (μ-oxo)bis(μ-carboxylato)diiron(III) complexes.[13] The success of this method is attributed largely to the remarkable ability of XDK^{2-} to support and stabilize dicarboxylate-bridged dimetallic centers, which we have demonstrated through a series of studies.[14−21]

We report here the synthesis of the neutral (μ-oxo)bis(μ-carboxylato)diiron(III) complex $[Fe_2(\mu\text{-}O)(\mu\text{-}XDK)(hfac)_2(H_2O)_2]$ (**3**), where $hfac^- = 1,1,1,5,5,5$-hexafluoroacetylacetonate, and its protonated (μ-hydroxo)bis(μ-carboxylato)diiron(III) analogue $[Fe_2(\mu\text{-}OH)(\mu\text{-}XDK)(hfac)_2(H_2O)_2]^+$ (**4**). The X-ray structural as well as optical and Mössbauer spectroscopic properties of **3** and **4** are presented. Furthermore, we show the importance of protonation to the EPR spectra of cryoreduced samples of well-defined (μ-oxo)- and (μ-hydroxo)bis(μ-carboxylato)diiron(III) complexes. The results from these experiments are explained in terms of the presence of either a bridging oxide or hydroxide in these compounds.

Experimental Section

General Methods. The compounds $[Fe_2(\mu\text{-}O)(\mu\text{-}XDK)(CH_3OH)_5(H_2O)](NO_3)_2$ (**5**)[10] and sodium tetrakis(3,5-bis(trifluoromethyl)phenyl)borate ($NaBAr_F$)[22] were synthesized according to literature procedures. Solutions of **2** were obtained by dissolving compound **5** in methanol.[10]

$[Fe_2(\mu\text{-}O)(\mu\text{-}XDK)(hfac)_2(H_2O)_2]$ (3). To a forest green solution of **2** (0.069 mmol in 2.5 mL of MeOH) was added dropwise with stirring a methanolic solution (1.5 mL) of 1,1,1,5,5,5-hexafluoroacetylacetone (hfacH) (19.5 μL, 0.138 mmol) and Et_3N (19.2 μL, 0.138 mmol). The resulting olive green solution was evaporated to dryness to yield a green solid, which was subsequently extracted with 1:1 CH_3CN/Et_2O (5 mL). This mixture was filtered and the filtrate evaporated. Recrystallization of the resulting solid from $CH_3CN/Et_2O/H_2O$ by slow evaporation produced dark green crystals, which were washed with cold (−20 °C) acetonitrile and dried in air to yield **3** as a green powder (59 mg, 74%). FTIR (cm^{-1}, KBr pellet): 3437 (br), 2968, 2936, 1728, 1685, 1652, 1548, 1467, 1410, 1363, 1263, 1199, 1146. Anal. Calcd for $C_{42}H_{44}N_2O_{15}F_{12}Fe_2$: C, 43.62; H, 3.83; N, 2.42. Found: C, 43.94; H, 3.72; N, 2.42.

$[Fe_2(\mu\text{-}OH)(\mu\text{-}XDK)(hfac)_2(H_2O)_2]BAr_F$ (4(BAr_F)). To a solution of **2** (0.11 mmol in 4 mL of MeOH) was added slowly with stirring neat hfacH (31 μL, 0.22 mmol), causing the color of the solution to change from dark green to orange. Subsequent addition of a solution of $NaBAr_F$ (100 mg, 0.113) in methanol (2 mL) followed by evaporation of the solvent under vacuum yielded an orange solid. To a mixture of this material in chlorobenzene (5 mL) was added the minimal amount of acetone required to effect complete dissolution of the product. The orange solution was filtered, and the filtrate was allowed to evaporate slowly in air for a few days, during which time orange needles precipitated. The crystals were harvested, washed with hexanes, and then dried in air. The resulting solid was pulverized and dried under vacuum to yield **4**(BAr_F) as an orange powder (193 mg, 86%). The aqua ligands of **4** are presumed to derive from adventitious water contained in the solvents. FTIR (cm^{-1}, KBr pellet): 3375 (br), 2981, 2942, 1723, 1675, 1646, 1625, 1542, 1357, 1282, 1255, 1226, 1164, 1132. Anal. Calcd for $C_{74}H_{57}N_2O_{15}F_{36}BFe_2$: C, 43.99; H, 2.84; N, 1.39. Found: C, 43.76; H, 2.88; N, 1.38.

Table 1. X-ray Crystallographic Information for $[Fe_2(\mu\text{-}O)(\mu\text{-}XDK)(hfac)_2(H_2O)_2]\cdot H_2O\cdot 1.5CH_3CN$ ($3\cdot H_2O\cdot 1.5CH_3CN$)

formula	$C_{45}H_{50.5}N_{3.5}O_{16}F_{12}Fe_2$
fw	1236.09
cryst size, mm	0.5 × 0.4 × 0.1
cryst system	Triclinic
space group	$P\bar{1}$
T, °C	−85
a, Å	13.9442(3)
b, Å	15.2151(4)
c, Å	15.7164(3)
α, deg	109.032(1)
β, deg	97.975(1)
γ, deg	115.697(1)
V, Å^3	2682.4(1)
Z	2
ρ_{calcd}, g cm^{-3}	1.530
abs coeff, mm^{-1}	0.651
effective transm factor	0.502−1.00
2θ range, deg	$2.90 \le 2\theta \le 56.66$
no. of data	11 687
no. of param	715
R1[a] ($I > 2\sigma(I)$)	0.0476
wR2[b] ($I > 2\sigma(I)$)	0.1312

[a] $R1 = \Sigma||F_o| - |F_c||/\Sigma|F_o|$. [b] $wR2 = \{\Sigma[w(F_o^2 - F_c^2)^2]/\Sigma[w(F_o^2)^2]\}^{1/2}$.

X-ray Crystallography. Recrystallization of **3** by slow evaporation of a solution containing a 4:2:0.05 $CH_3CN/Et_2O/H_2O$ solvent mixture at room temperature yielded X-ray-quality crystals of $3\cdot H_2O\cdot 1.5CH_3CN$. A single crystal was mounted in Paratone N oil on the end of a glass fiber and then frozen into place under a low-temperature nitrogen cold stream set at −85 °C. Data were collected on a Siemens SMART/CCD X-ray diffractometer with Mo Kα radiation (λ = 0.710 73 Å). Details of the data collection and reduction protocols are described elsewhere.[23] The structure was solved by direct methods and refined on F^2 by using the SHELXTL software package. All non-hydrogen atoms except those of the acetonitrile molecules were refined anisotropically. Empirical absorption corrections were applied by using the SADABS program. Hydrogen atoms were assigned idealized positions and isotropic thermal parameters equivalent to either 1.5 (methyl hydrogens) or 1.2 (all other hydrogens) times the thermal parameter of the carbon atom to which they were attached. The hydrogens associated with the water and acetonitrile molecules were not included in the refinement. Both lattice acetonitrile molecules exhibited disorder; one was refined at half-occupancy and the other at full occupancy divided equally over three positions. Relevant crystallographic information is listed in Tables 1 and 2.

Cryogenic Reduction. Complexes **3** and **4** were prepared as 2−5 mM solutions in either 2:1 acetone/CH_3CN or 2-methyltetrahydrofuran (2-MeTHF). The samples were frozen in liquid nitrogen in 3-mm i.d. quartz tubes and exposed to γ-radiation from a ^{60}Co source for a total dose of 2.5−4 Mrad at a rate of 0.46 Mrad h^{-1}. Annealing was performed by incubating the cryogenically reduced samples in a cold isopentane bath, after which the samples were cooled rapidly back down to 77 K.

(13) Mizoguchi, T. J.; Lippard, S. J. *Inorg. Chem.* **1997**, *36*, 4526−4533.
(14) Goldberg, D. P.; Koulougliotis, D.; Brudvig, G. W.; Lippard, S. J. *J. Am. Chem. Soc.* **1995**, *117*, 3134−3144.
(15) Tanase, T.; Lippard, S. J. *Inorg. Chem.* **1995**, *34*, 4682−4690.
(16) Tanase, T.; Yun, J. W.; Lippard, S. J. *Inorg. Chem.* **1996**, *35*, 3585−3594.
(17) Yun, J. W.; Tanase, T.; Lippard, S. J. *Inorg. Chem.* **1996**, *35*, 7590−7600.
(18) Herold, S.; Lippard, S. J. *J. Am. Chem. Soc.* **1997**, *119*, 145−156.
(19) LeCloux, D. D.; Lippard, S. J. *Inorg. Chem.* **1997**, *36*, 4035−4046.
(20) He, C.; Lippard, S. J. *J. Am. Chem. Soc.* **1998**, *120*, 105−113.
(21) LeCloux, D. D.; Davydov, R.; Lippard, S. J. *Inorg. Chem.* **1998**, *37*, 6814−6826.
(22) Brookhart, M.; Grant, B.; Volpe, A. F., Jr. *Organometallics* **1992**, *11*, 3920−3922.
(23) Feig, A. L.; Bautista, M. T.; Lippard, S. J. *Inorg. Chem.* **1996**, *35*, 6892−6898.

Table 2. Selected Bond Distances (Å) and Angles (deg) for $[Fe_2(\mu\text{-}O)(\mu\text{-}XDK)(hfac)_2(H_2O)_2]\cdot H_2O\cdot 1.5CH_3CN$ $(3\cdot H_2O\cdot 1.5CH_3CN)$[a,b]

Bond Distances			
Fe1−O1	1.792(2)	Fe2−O1	1.796(2)
Fe1−O101	2.024(2)	Fe2−O102	2.021(2)
Fe1−O201	2.026(2)	Fe2−O202	2.014(2)
Fe1−O2	2.074(2)	Fe2−O4	2.061(2)
Fe1−O3	2.078(2)	Fe2−O5	2.079(2)
Fe1−O6	2.133(2)	Fe2−O7	2.099(2)
Bond Angles			
Fe1−O1−Fe2	124.82(9)	O1−Fe2−O102	93.26(7)
O1−Fe1−O101	94.23(7)	O1−Fe2−O202	94.38(7)
O1−Fe1−O201	94.17(7)	O1−Fe2−O4	98.48(8)
O1−Fe1−O2	95.62(8)	O1−Fe2−O5	96.24(8)
O1−Fe1−O3	96.69(8)	O1−Fe2−O7	177.55(7)
O1−Fe1−O6	178.29(8)	O4−Fe2−O102	87.29(7)
O2−Fe1−O101	167.03(8)	O4−Fe2−O202	164.98(8)
O2−Fe1−O201	87.16(8)	O4−Fe2−O5	84.06(7)
O2−Fe1−O3	84.15(8)	O4−Fe2−O7	83.84(8)
O2−Fe1−O6	84.01(8)	O5−Fe2−O102	167.99(8)
O3−Fe1−O101	86.33(7)	O5−Fe2−O202	86.87(7)
O3−Fe1−O201	166.69(7)	O5−Fe2−O7	84.74(8)
O3−Fe1−O6	84.93(8)	O7−Fe2−O102	86.06(8)
O6−Fe1−O101	86.40(7)	O7−Fe2−O202	83.42(7)
O6−Fe1−O201	84.15(7)	O102−Fe2−O202	99.74(7)
O101−Fe1−O201	100.54(7)		

[a] See Figure 1 for the atom-labeling scheme. [b] Numbers in parentheses are estimated standard deviations for the last significant digit.

Spectroscopy. Optical and FTIR spectra were recorded on an HP 8452 diode array spectrophotometer and a Bio-Rad FTS 135 spectrometer, respectively. Mössbauer spectra were measured at 77 K by using a room temperature ^{57}Co source in a Rh matrix and fit to Lorentzian line shapes. Isomer shifts were referenced to natural abundance Fe metal at room temperature. Powdered material was suspended in Apiezon N grease and then spread evenly into nylon sample holders. X-band EPR spectra were recorded on Bruker ESP300 and EMX spectrometers equipped with an Oxford Instrument ESR 900 liquid helium cryostat. The field modulation was set at 100 kHz.

Results and Discussion

Synthesis. Addition of 2 equiv of hfacH and Et_3N to a solution of **2** in methanol led to displacement of two solvent ligands with an anionic $hfac^-$ at each iron center of the (μ-oxo)(μ-XDK)diiron(III) starting material. The initially formed olive green adduct contains one methanol ligand per iron, but recrystallization of this crude product from a $CH_3CN/Et_2O/H_2O$ solvent mixture yielded upon drying the neutral bis(aqua) compound $[Fe_2(\mu\text{-}O)(\mu\text{-}XDK)(hfac)_2(H_2O)_2]$ (**3**). In contrast, when 2 equiv of hfacH was allowed to react with **2** in methanol in the absence of an external base, the color of the reaction mixture turned orange. This color is ascribed to the formation of a cationic (μ-hydroxo)(μ-XDK)diiron(III) complex in which the counteranion is nitrate and the proton of the hydroxide bridge derives from ionization of hfacH.

This protonation process is reversible since subsequent addition of Et_3N to the orange solution of the cation generated a green solution, resulting from the deprotonation of the hydroxo bridge to form the corresponding μ-oxo derivative. Furthermore, green methanolic solutions of **3** could be converted to its orange protonated analogue with Brønsted acids such as HCl, HNO_3, and $HClO_4$. To obtain stable and analytically pure samples of the μ-hydroxo derivative, we tested the potential utility of noncoordinating counteranions such as tetraphenylborate (BPh_4^-) and tetrakis(3,5-bis(trifluoromethyl)phenyl)borate (BAr_F^-). Addition of $NaBPh_4$ to an orange solution, generated from the reaction of **2** with 2 equiv of hfacH in methanol, led to immediate conversion to a dark red solution of unknown composition. This apparent decomposition pathway was avoided, however, by using $NaBAr_F$ in which case the orange color of the solution was retained after its addition. Recrystallization of this orange material from chlorobenzene/acetone afforded upon drying $[Fe_2(\mu\text{-}OH)(\mu\text{-}XDK)(hfac)_2(H_2O)_2]BAr_F$ (**4**(BAr_F)) in high yields.

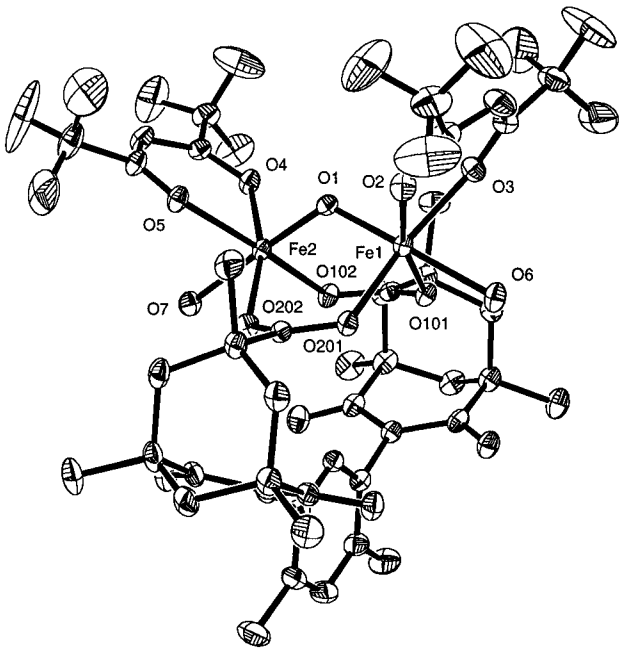

Figure 1. ORTEP diagram of $[Fe_2(\mu\text{-}O)(\mu\text{-}XDK)(hfac)_2(H_2O)_2]$ (**3**), showing 40% probability thermal ellipsoids for all non-hydrogen atoms.

The (μ-oxo)bis(μ-carboxylato)diiron(III) complex $[Fe_2(\mu\text{-}O)(\mu\text{-}O_2CCH_3)_2(HBpz_3)_2]$ (**6**), where $HBpz_3^-$ = hydrotris(pyrazolyl)borate,[24] has been demonstrated previously to exhibit reversible protonation behavior, and the hydroxo-bridged analogue $[Fe_2(\mu\text{-}OH)(\mu\text{-}O_2CCH_3)_2(HBpz_3)_2]^+$ (**7**) could be obtained as a perchlorate salt.[25] In both this system and the one presented here, coordination of anionic ligands, $hfac^-$ or $HBpz_3^-$, apparently increases the basicity of the bridging oxo group to a sufficient degree that the corresponding μ-hydroxo complex can not only be accessed but also isolated as a stable solid. The $HBpz_3^-$ ligand has also been used to synthesize oxo- and hydroxo-bridged pairs of diiron(III) compounds containing two additional bridges provided by either diphenyl phosphate or diphenylphosphinate groups.[26]

X-ray Crystallography. The single-crystal X-ray structure of compound **3** revealed the presence of two chemically equivalent iron coordination spheres that are related by a noncrystallographic 2-fold symmetry axis (Figure 1). The metal centers are triply bridged by two carboxylate groups provided by the XDK^{2-} ligand and an oxygen atom of an oxo group. The general structural features of the (μ-oxo)bis(μ-carboxylato)diiron core of **3**, with an Fe···Fe separation of 3.1794(5) Å, average $Fe-O_{bridge}$ bond distance of 1.794(2) Å, and $Fe-O_{bridge}-Fe$ bond angle of 124.82(9)°, are essentially identical to those of previously reported (μ-oxo)(μ-XDK)diiron(III) complexes.[10,13] A pseudo-octahedral geometry about each iron

(24) Armstrong, W. H.; Spool, A.; Papaefthymiou, G. C.; Frankel, R. B.; Lippard, S. J. *J. Am. Chem. Soc.* **1984**, *106*, 3653−3667.
(25) Armstrong, W. H.; Lippard, S. J. *J. Am. Chem. Soc.* **1984**, *106*, 4632−4633.
(26) Turowski, P. N.; Armstrong, W. H.; Liu, S.; Brown, S. N.; Lippard, S. J. *Inorg. Chem.* **1994**, *33*, 636−645.

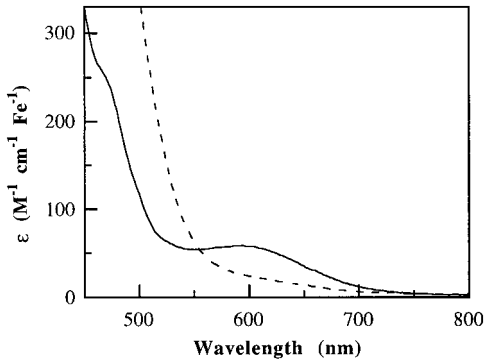

Figure 2. Visible absorption spectra of $[Fe_2(\mu\text{-}O)(\mu\text{-}XDK)(hfac)_2(H_2O)_2]$ (**3**) (—) and $[Fe_2(\mu\text{-}OH)(\mu\text{-}XDK)(hfac)_2(H_2O)_2]BAr_F$ (**4**(BAr_F)) (- - -) recorded at room temperature in methanol and 2:1 acetone/CH_3CN, respectively.

center is completed by coordination of a bidentate $hfac^-$ chelate and a terminal water molecule. Both oxygen donor atoms of each $hfac^-$ ligand are located cis to the oxo bridge, in contrast to the cis,trans arrangement of the nitrogen donor atoms of the bidentate bipyridyl ligands in related (μ-oxo)(μ-XDK)bis(2,2′-bipyridyl)diiron(III) complexes.[10,13] As a consequence, the water ligands of **3** are situated trans to the oxo bridge, an orientation that is preserved upon their replacement with other donors such as methanol and pyridine, as demonstrated by crystallographic chemical analysis.[27]

An X-ray structure of **4**(BAr_F) was also determined[28] by using crystals obtained directly from the synthetic procedure, but severe disorder in the lattice solvent molecules and the trifluoromethyl groups of the $hfac^-$ ligands and BAr_F^- counterion prevents its detailed discussion. Although the overall structure of complex **4** is very similar to that of **3**, protonation of the oxo bridge in the latter is accompanied by significant alterations to the diiron core structure. The average $Fe-O_{bridge}$ bond distance lengthens to 1.935(6) Å, an increase that reflects the poorer donor strength of a hydroxo versus an oxo ligand. The Fe···Fe separation also increases to 3.394(2) Å in **4**, but the $Fe-O_{bridge}-Fe$ bond angle remains almost unchanged at 122.6(3)°. The core metrical features of **3** and **4** agree with those of **6** and **7**,[25] respectively, and these two pairs of compounds constitute the only well-characterized examples of (μ-oxo/hydroxo)bis(μ-carboxylato)diiron(III) complexes that differ by the protonation state of the bridging oxygen atom.

Absorption Spectroscopy. The optical spectrum of **3** in methanol exhibits a broad transition centered ~590 nm and a shoulder ~460 nm (Figure 2). A relatively strong set of signals between ~300 and 400 nm is also observed where oxo-to-iron(III) charge-transfer and high-energy ligand-field bands of (μ-oxo)diiron(III) units are expected to occur.[9] It is likely that dissolution in this solvent is accompanied by rapid ligand exchange of the terminal water ligands, and we therefore attribute the observed spectrum to $[Fe_2(\mu\text{-}O)(\mu\text{-}XDK)(hfac)_2(CH_3OH)_2]$. The visible absorption features are assigned to ligand-field bands characteristic of high-spin pseudo-octahedral iron(III) centers, and their unusually high intensities are associated with the presence of an oxo-bridged diiron(III) moiety.[29] Furthermore, the position of the $^6A_1 \rightarrow [^4T_2]({}^4G)$ band (590 nm) is close to that observed in compound **1** (569 nm),[8] consistent with the weak ligand-field afforded by an all-oxygen-donor atom set. The corresponding d−d bands of compound **4** are expected to be very weak and are not observed in acetone/CH_3CN because they are obscured by an intense near-UV band that tails into the visible region (Figure 2). Solvents such as THF and 2-MeTHF apparently promote partial dissociation of the proton from the bridging hydroxide group of **4** as evidenced by the appearance of an absorption feature ~600 nm (data not shown), which is characteristic of the (μ-oxo)diiron(III) chromophore.[29]

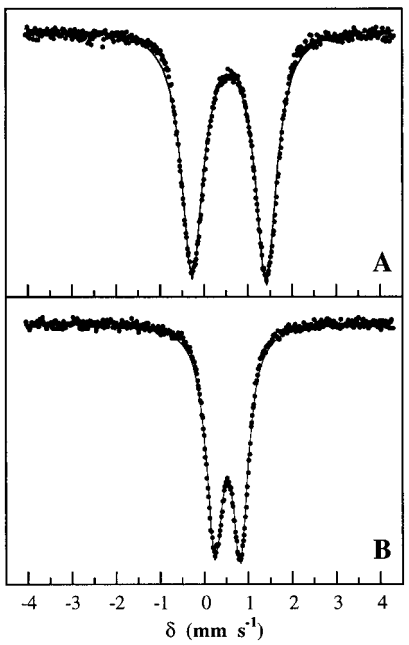

Figure 3. Mössbauer spectra of $[Fe_2(\mu\text{-}O)(\mu\text{-}XDK)(hfac)_2(H_2O)_2]$ (**3**) (A) and $[Fe_2(\mu\text{-}OH)(\mu\text{-}XDK)(hfac)_2(H_2O)_2]BAr_F$ (**4**(BAr_F)) (B) recorded at 77 K.

The UV−vis spectra of compounds **3** and **4** share features similar to those of the μ-oxo compound **6** and μ-hydroxo compound **7**,[25] respectively. Both systems clearly demonstrate the sensitivity of the electronic structures of diiron(III) compounds to the protonation state of a single-atom oxygen bridge. The near-UV absorption in **7** has been assigned to a $HBpz_3^-$-to-iron(III) charge-transfer transition,[26] and by analogy, the near-UV absorption in **4** is tentatively assigned to a $hfac^-$-to-iron(III) charge-transfer transition. The corresponding ligand-to-metal charge-transfer band in the oxo-bridged compound **3** is presumably shifted to higher energy owing to the greater electrostatic stabilization of the iron(III) oxidation state provided by an oxo versus a hydroxo ligand.

Mössbauer Spectroscopy. The 77 K Mössbauer spectrum of **3** is characterized by a symmetric quadrupole doublet with $\delta = 0.58$ and $\Delta E_Q = 1.68$ mm s^{-1} (Figure 3A), a result that is consistent with the chemical equivalence of the two iron centers. The isomer shift is indicative of high-spin iron(III), whereas the unusually large quadrupole splitting value is consistent with the presence of a bridging oxo group,[9] which induces a relatively large electric field gradient at the iron nuclei. The 77 K Mössbauer spectrum of **4**(BAr_F) also appears as a symmetric quadrupole doublet with a very similar δ of 0.53 mm s^{-1} but a considerably decreased ΔE_Q value of 0.58 mm s^{-1} (Figure 3B). Protonation of the oxo bridge in compound **3** is not accompanied by a change in the iron oxidation or spin state and, hence, has little effect on the isomer shift. In contrast, the presence of a hydroxo bridge in compound **4** affords a more symmetric

(27) Mizoguchi, T. J.; Lippard, S. J. Unpublished results.
(28) Crystal data: monoclinic, $P2_1/n$, $a = 16.0965(4)$ Å, $b = 24.0066(6)$ Å, $c = 24.8125(6)$ Å, $\beta = 91.967(1)°$, $V = 9582.5(4)$ Å^3, $Z = 4$, $T = -85$ °C.
(29) Reem, R. C.; McCormick, J. M.; Richardson, D. E.; Devlin, F. J.; Stephens, P. J.; Musselman, R. L.; Solomon, E. I. *J. Am. Chem. Soc.* **1989**, *111*, 4688−4704.

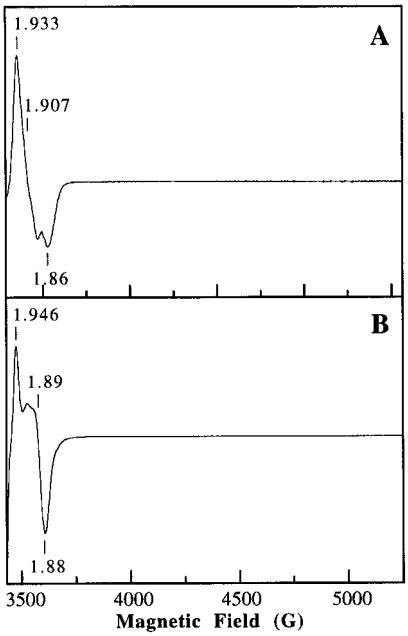

Figure 4. X-band EPR spectra of $[Fe_2(\mu\text{-O})(\mu\text{-XDK})(hfac)_2(H_2O)_2]$ (**3**) reduced radiolytically at 77 K in 2:1 acetone/CH_3CN (A) and 2-MeTHF (B) glasses. Spectra were recorded at 30 and 77 K, respectively. Instrument settings: amplitude modulation 5 G; gain 5000; 1-mW power at 9.424 GHz. Radical signals induced by γ-radiolysis are omitted for clarity.

coordination environment, in particular with respect to the bond distances to the distorted octahedral iron center (vide supra). This situation translates into a relatively small electric field gradient and a quadrupole splitting that is more typical of mononuclear, six-coordinate, high-spin iron(III) complexes.

EPR Spectroscopy. A cryogenic reduction technique has been applied to generate kinetically stabilized mixed-valence $Fe^{II}Fe^{III}$ forms of complexes **3** and **4**. Previous work has shown that the diiron(III) sites in proteins and model compounds can be reduced efficiently by one electron with yields of 30−70% in frozen solution at 77 K by utilizing mobile electrons generated by γ-irradiation.[30] Due to low molecular mobility in frozen solutions at 77 K, the mixed-valence species will retain a coordination structure close to that of the original diiron(III) form. The conformation of the mixed-valent state will therefore be trapped in a nonequilibrium state. If the structure of the complex depends on the redox state of the iron atom(s), this primary product will then relax to thermodynamically more stable adducts at higher temperatures, ∼120−160 K for diiron complexes of the type discussed here.[30]

The mixed-valence form of complex **3**, generated in an acetone/CH_3CN glass at 77 K, shows a rhombic $g < 2$ EPR signal with effective *g*-values of 1.933, 1.907, and 1.86 (Figure 4A). A slightly different EPR spectrum is obtained when γ-radiolysis of the same compound is performed in a 2-MeTHF glass (Figure 4B). This observation is attributed to differences in the identity of the ligands trans to the oxo bridge in these two solvent systems. The substitutional lability of the terminal water ligands in **3** has been discussed above. The shape of the mixed-valence signals presented in Figure 3A,B is independent of temperature from 5 to 100 K. The EPR properties of the mixed-valence form of **3** trapped at 77 K are consistent with those reported for other oxo-bridged $Fe^{II}Fe^{III}$ units produced under similar conditions.[30]

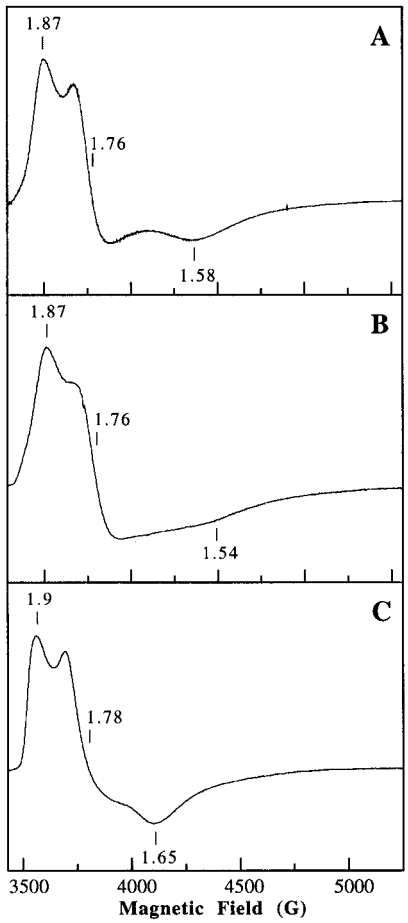

Figure 5. X-band EPR spectra recorded at 4.2 K of $[Fe_2(\mu\text{-OH})(\mu\text{-XDK})(hfac)_2(H_2O)_2]^+$ (**4**) reduced radiolytically at 77 K in a 2:1 acetone/CH_3CN glass (A) and after annealing at 120 K for 1 min (B) and of cryogenically reduced $[Fe_2(\mu\text{-O})(\mu\text{-XDK})(hfac)_2(H_2O)_2]$ (**3**) in a 2-MeTHF glass after annealing at 140 K for 1 min (C). Instrument settings: amplitude modulation 10 G; gain 5000; 1-mW microwave power at 9.42 GHz. Radical signals induced by γ-radiolysis are omitted for clarity.

A sample of **4** cryoreduced in an acetone/CH_3CN glass shows a substantially anisotropic EPR signal with effective *g*-values of 1.87, 1.76, and 1.58 (Figure 5A), which is observable below 20 K. Since complex **4** converts partially to **3** in 2-MeTHF, the cryoreduction experiment in this solvent has not been performed. The striking contrast in the *g*-anisotropy and relaxation behavior of the EPR signals of the mixed-valence $Fe^{II}Fe^{III}$ species derived from oxo- and hydroxo-bridged diiron(III) complexes reflects mainly the difference in antiferromagnetic exchange coupling between the iron(II) and iron(III) centers that leads to an $S = {}^1/_2$ ground state. The relatively strong coupling afforded by the oxo group in cryogenically reduced **3** yields a narrow spread in *g*-values, whereas the weaker coupling provided by the hydroxo bridge in **4** results in a significant increase in **g**-tensor anisotropy.[31−34]

(30) Davydov, R. M.; Ménage, S.; Fontecave, M.; Gräslund, A.; Ehrenberg, A. *JBIC* **1997**, *2*, 242−255.

(31) Sage, J. T.; Xia, Y.-M.; Debrunner, P. G.; Keough, D. T.; de Jersey, J.; Zerner, B. *J. Am. Chem. Soc.* **1989**, *111*, 7239−7247.

(32) Rodriguez, J. H.; Ok, H. N.; Xia, Y.-M.; Debrunner, P. G.; Hinrichs, B. E.; Meyer, T.; Packard, N. H. *J. Phys. Chem.* **1996**, *100*, 6849−6862.

(33) McCormick, J. M.; Reem, R. C.; Solomon, E. I. *J. Am. Chem. Soc.* **1991**, *113*, 9066−9079.

(34) Fox, B. G.; Hendrich, M. P.; Surerus, K. K.; Andersson, K. K.; Froland, W. A.; Lipscomb, J. D.; Münck, E. *J. Am. Chem. Soc.* **1993**, *115*, 3688−3701.

Annealing of the low-temperature reduced samples of **3** and **4** at 120−145 K for 1 min alters the mixed-valence EPR signals. The EPR spectrum of cryogenically reduced **4** changes only slightly upon annealing at 144 K (Figure 5A,B). The observed alterations are probably due to redox-induced ligand reorientation. In contrast, new anisotropic signals exhibiting a large spread in *g*-values are observed after annealing at 144 K mixed-valence **3** trapped at 77 K in an acetone/CH_3CN glass (Figure 5C). This spectrum appears very similar to that of the relaxed form of the mixed-valence derivative of **4** (Figure 5B) where the observed disparities can be ascribed to solvent-derived differences in the ligands trans to the bridging oxygen atom (vide supra). This result suggests that, upon warming, the initially formed (μ-oxo)$Fe^{II}Fe^{III}$ adduct, which is generated in a nonequilibrium state, converts to the corresponding (μ-hydroxo)$Fe^{II}Fe^{III}$ species by reaction with an adventitious source of protons in the solvent. Reduction of the diiron(III) center in **3** is apparently associated with a decrease in the overall Lewis acidity of the dinuclear site and, therefore, an apparent increase in the basicity of the bridging oxo group.

Conclusion

A pair of bis(μ-carboxylato)diiron(III) complexes that differ only by the presence of either a bridging oxo or hydroxo ligand has been synthesized and characterized. Coordination by a bidentate $hfac^-$ anion to each of the iron centers of the dicationic (μ-oxo)bis(μ-carboxylato)diiron(III) complex **2** generates a neutral compound bearing a bridging oxo group that can be protonated in a reversible fashion. The general structural features of $[Fe_2(\mu\text{-}O)(\mu\text{-}XDK)(hfac)_2(H_2O)_2]$ (**3**) and $[Fe_2(\mu\text{-}OH)(\mu\text{-}XDK)(hfac)_2(H_2O)_2]^+$ (**4**) are very similar, although significant metrical differences occur in the $\{Fe-O(H)-Fe\}^{4(5)+}$ unit. The optical, Mössbauer, and cryoreduced EPR spectroscopic properties of **3** and **4** are distinct from one another and can be correlated to the protonation state of the oxygen atom that bridges the two iron centers and, hence, the degree of communication that exists between the two high-spin metal ions. These results provide useful points of comparison for understanding the nature of less well-defined diiron(III) centers in both proteins and models.

Acknowledgment. This work was supported by a grant from the National Science Foundation. T.J.M. thanks the NIH for a postdoctoral fellowship. We are grateful to Prof. W. M. Reiff of Northeastern University for allowing us to use his Mössbauer spectrometer.

Supporting Information Available: Tables of X-ray crystallographic data, an ORTEP diagram, and CIF data for compound **3**. This material is available free of charge via the Internet at http://pubs.acs.org.

IC990303Y